

Supramolecular assembly and structural transformation of d¹⁰-metal complexes containing (aza-15-crown-5)dithiocarbamate

Biing-Chiau Tzeng,^{*,a} Chung-Lun Wu,^a Jun-Wei Hung,^a Su-Ying Chien^b and Gene-Hsiang Lee^b

^aDepartment of Chemistry and Biochemistry, National Chung Cheng University, 168 University Road, Min-Hsiung, Chiayi 62102, Taiwan

^bDepartment of Chemistry, National Taiwan University, 1, Sec. 4, Roosevelt Road, Taipei 10617, Taiwan

Table S1 Crystallographic Data of **1-6**.

	1	2	2'	3	4	5	6
Empirical formula	C ₁₁ H ₂₀ AgNO ₄ S ₂	C ₅₂ H ₉₂ Cu ₄ N ₈ O ₁₆ S ₈	C ₈₈ H ₁₆₀ Cu ₈ N ₈ O ₃₂ S ₁₆	C ₂₂ H ₄₂ AgLiN ₂ O ₉ S ₄	C ₂₂ H ₄₀ AgN ₂ NaO ₈ S ₄	C ₂₂ H ₄₀ AgKN ₂ O ₈ S ₄	C ₂₂ H ₄₀ AgN ₂ O ₈ RbS ₄
Formula weight	402.27	1595.97	2863.51	721.62	719.66	735.77	782.14
Crystal system	Orthorhombic	Tetragonal	Triclinic	Triclinic	Monoclinic	Hexagonal	Hexagonal
Space group	Pccn	I-4	P-1	P-1	C2/c	P6 ₃ 22	P6 ₅ 22
a (Å)	16.7239(16)	19.5073(4)	13.0623(9)	10.0460(19)	31.430(6)	9.656(2)	9.70500(7)
b (Å)	21.489(3)	19.5073(4)	13.8962(10)	10.0552(19)	20.015(5)	9.656(2)	9.70500(7)
c (Å)	8.2014(9)	8.9948(2)	17.5548(12)	16.237(3)	18.982(4)	57.87(2)	58.1123(7)
α(°)	90	90	75.058(2)	93.574(2)	90	90	90
β(°)	90	90	79.229(2)	104.499(3)	95.95(2)	90	90
γ(°)	90	90	74.115(2)	96.368(2)	90	120	120
V (Å ³), Z	2947.5(6), 8	3422.83(16), 2	2937.9(4), 1	1571.2(5), 2	11877(5), 16	4672(3), 6	4740.12(9), 6
F(000) (e)	1632	1664	1488	748	5952	2280	2388
μ(Mo-Kα) (mm ⁻¹)	1.659	1.537	1.779	0.955	1.021	1.093	2.477
T (K)	100(2)	150(2)	150(2)	173(2)	173(2)	173(2)	150(2)
Reflections collected	13261	38501	53694	5583	44976	36217	43051
Independent reflections (R _{int} =0.056) (Fo ≥ 2σ(Fo))	2592	5003	13392	5583	13527	3589	4631
	(R _{int} =0.056)	(R _{int} =0.045)	(R _{int} =0.083)	(R _{int} =0.050)	(R _{int} =0.177)	(R _{int} =0.047)	(R _{int} =0.045)
Refined parameters	172	200	698	381	693	186	174
Goodness-of-fit on F ²	1.047	1.046	1.009	1.105	0.929	1.336	1.125
R ^a , R _w ^b (I ≥ 2σ(I))	0.0350, 0.0812	0.0178, 0.0414	0.0526, 0.1150	0.0925, 0.2254	0.0728, 0.1627	0.0648, 0.1479	0.0274, 0.0672
R ^a , R _w ^b (all data)	0.0457, 0.0882	0.0190, 0.0417	0.0934, 0.1371	0.1015, 0.2316	0.1918, 0.2123	0.0666, 0.1488	0.0287, 0.0677

$${}^aR = \frac{\sum ||F_o| - |F_c||}{\sum |F_o|}, \quad {}^bR_w = \left\{ \frac{\sum w(F_o^2 - F_c^2)^2}{\sum [w(F_o^2)]} \right\}^{1/2}.$$

Supporting Information

Figure S1. The packing diagram of complex **3** with each Li^+ ion of 50% disorder.

Figure S2. Experimental and simulated powder X-ray diffraction patterns of complex **1**.

Figure S3. Experimental and simulated powder X-ray diffraction patterns of complex **2**

Figure S4. Experimental and simulated powder X-ray diffraction patterns of complex **2'**.

Figure S5. Experimental and simulated powder X-ray diffraction patterns of complex **3**.

Figure S6. Experimental and simulated powder X-ray diffraction patterns of complex **4**.

Figure S7. Experimental and simulated powder X-ray diffraction patterns of complex **5**.

Figure S8. Experimental and simulated powder X-ray diffraction patterns of complex **6**.

Figure S9. The TGA trace of complex **1**.

Figure S10. The TGA trace of complex **2**.

Figure S11. The TGA trace of complex **2'**.

Figure S12. The TGA trace of complex **3**.

Figure S13. The TGA trace of complex **4**.

Figure S14. The TGA trace of complex **5**.

Figure S15. The TGA trace of complex **6**.

Figure S16. Luminescence spectra for solid samples of KO_4NCS_2 (orange line), complexes **1** (blue line), **2** (pink line), and **2'** (green line) and quartz disc (background : gray dash dotted line) at room temperature. The excitation wavelength is 350 nm.

Figure S17. Luminescence spectra for solid samples of KO_4NCS_2 (purple line), complexes **3** (red line), **4** (blue line), **5** (pink line), and **6** (green line) and quartz disc (background : gray dash dotted line) at room temperature. The excitation wavelength is 350 nm.

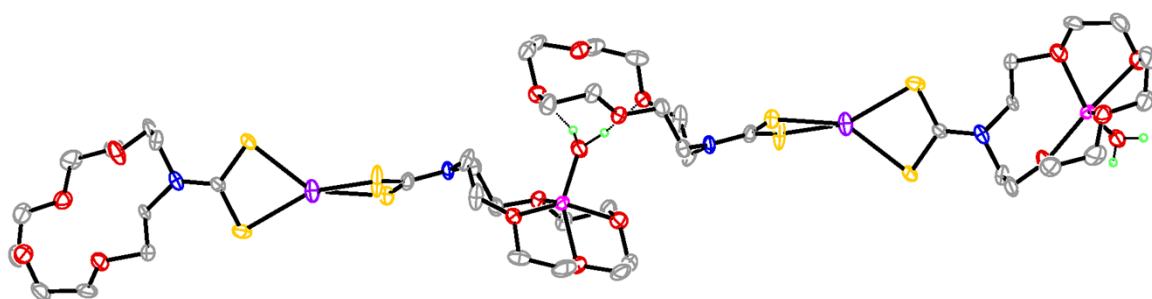


Figure S1. The packing diagram of complex **3** with each Li^+ ion of 50 % disorder.

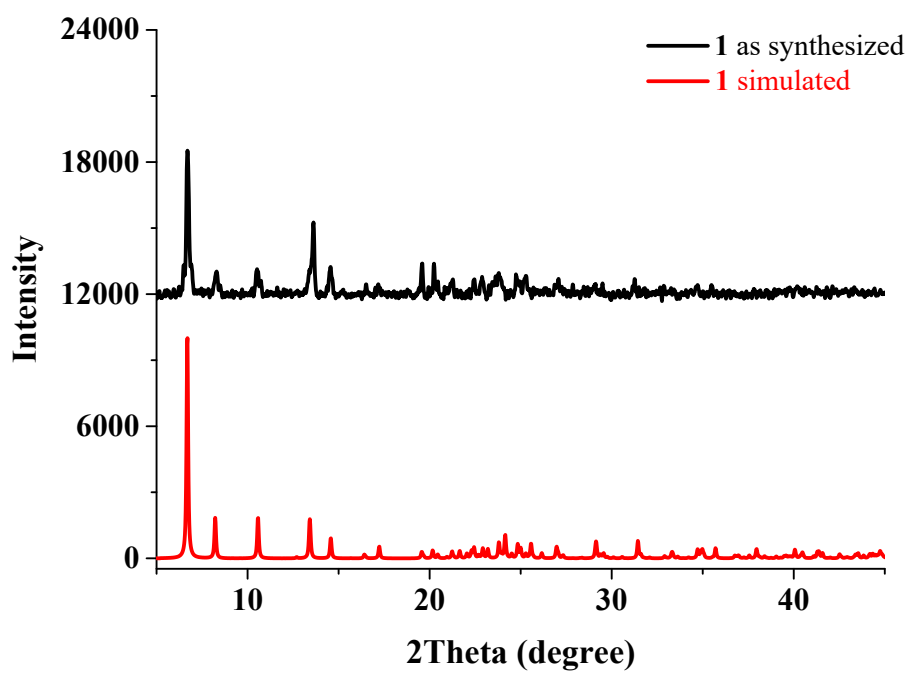


Figure S2. The experimental and simulated powder X-ray diffraction patterns of complex **1**.

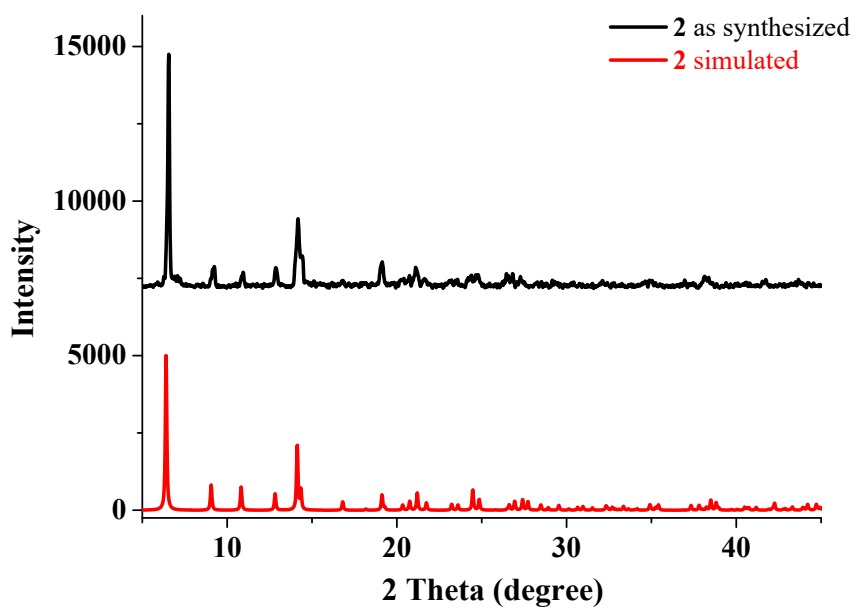


Figure S3. The experimental and simulated powder X-ray diffraction patterns of complex 2.

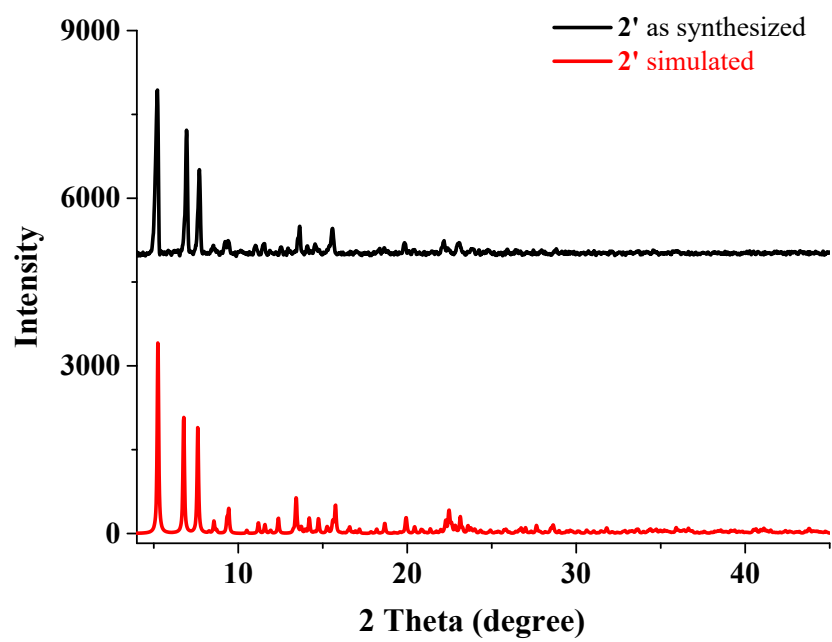


Figure S4. The experimental and simulated powder X-ray diffraction patterns of complex **2'**.

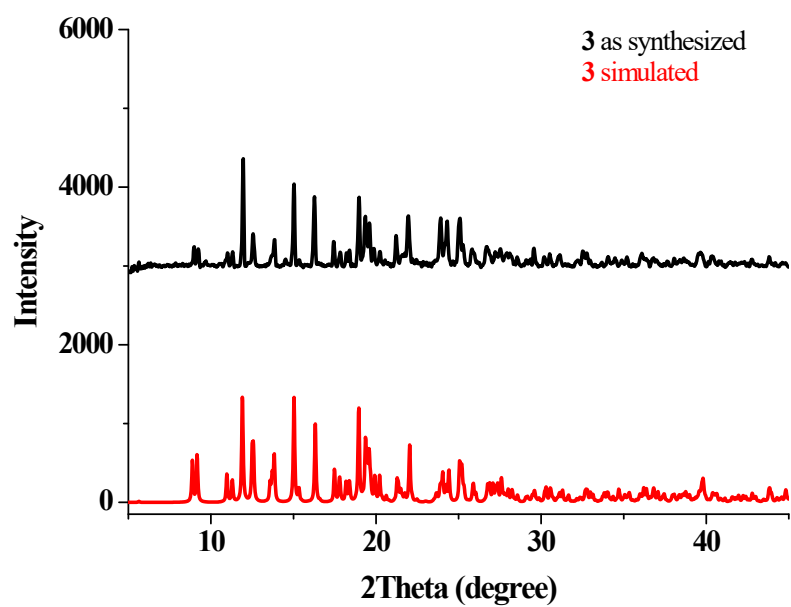


Figure S5. The experimental and simulated powder X-ray diffraction patterns of complex **3**.

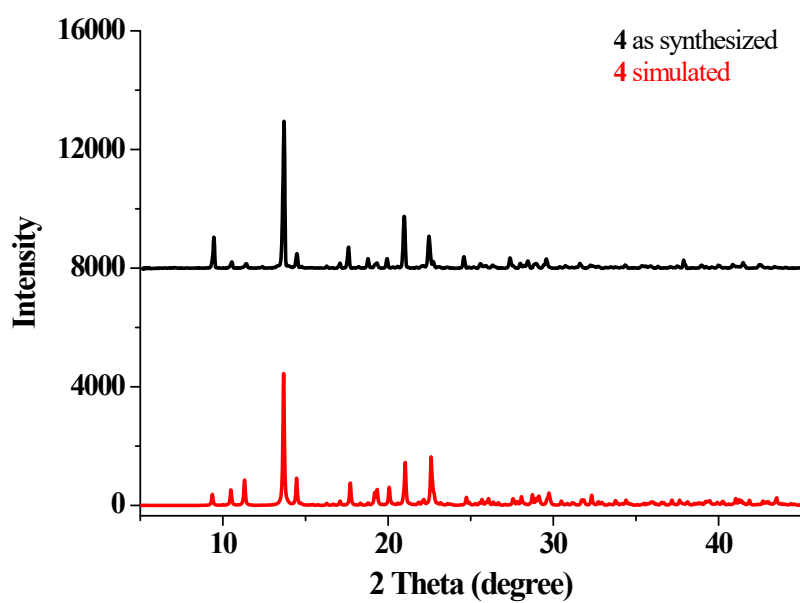


Figure S6. The experimental and simulated powder X-ray diffraction patterns of complex 4.

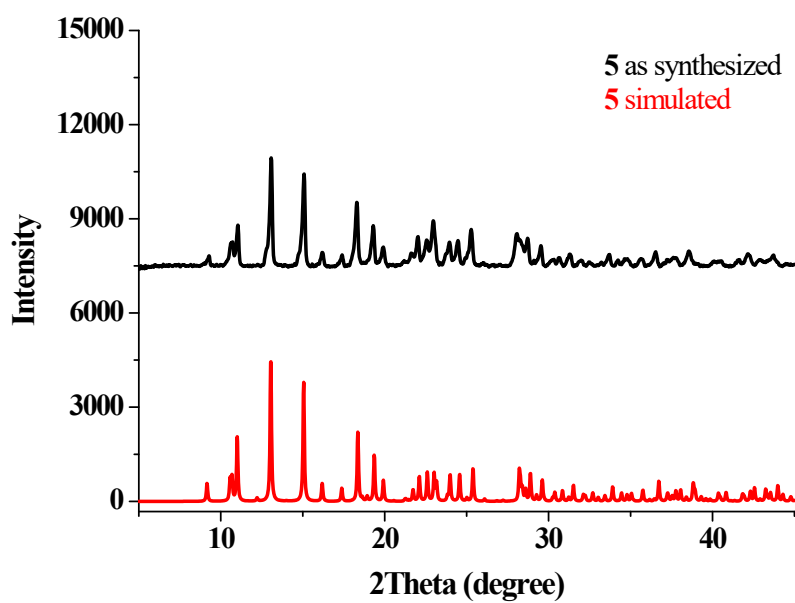


Figure S7. The experimental and simulated powder X-ray diffraction patterns of complex **5**.

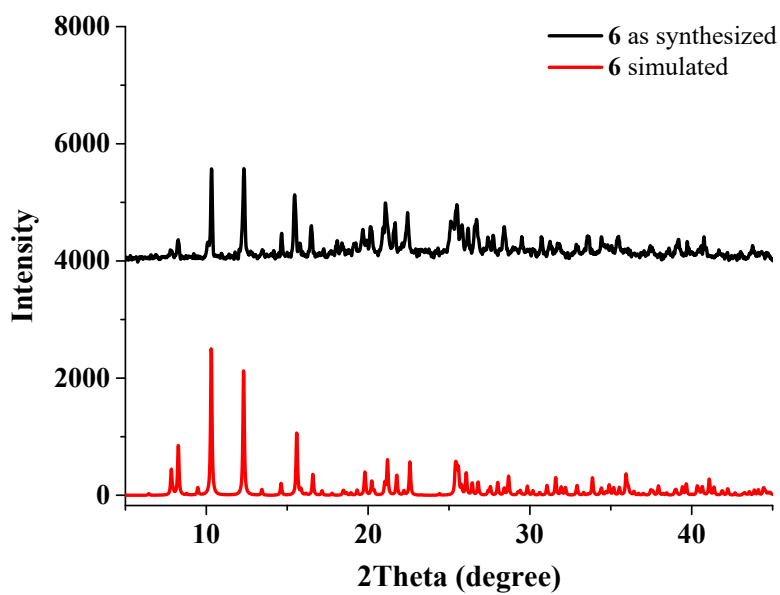


Figure S8. The experimental and simulated powder X-ray diffraction patterns of complex **6**.

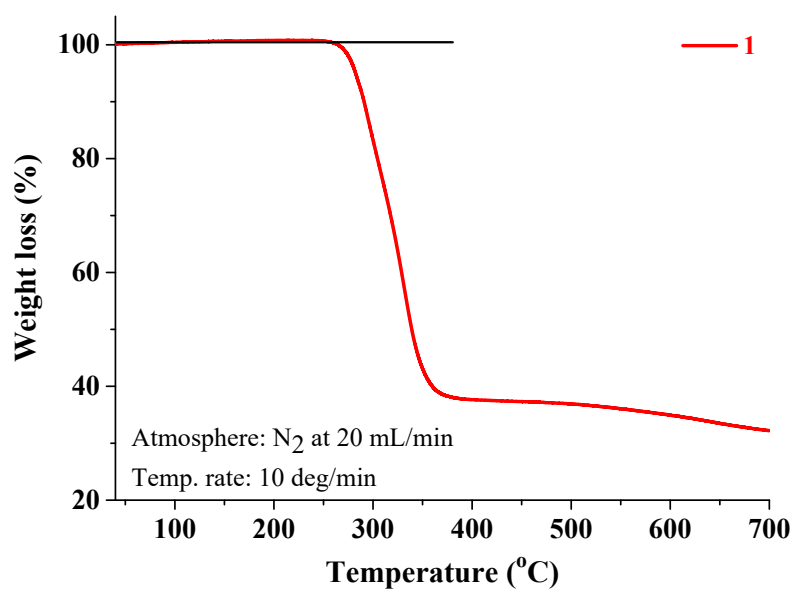


Figure S9. The TGA trace of complex **1**.

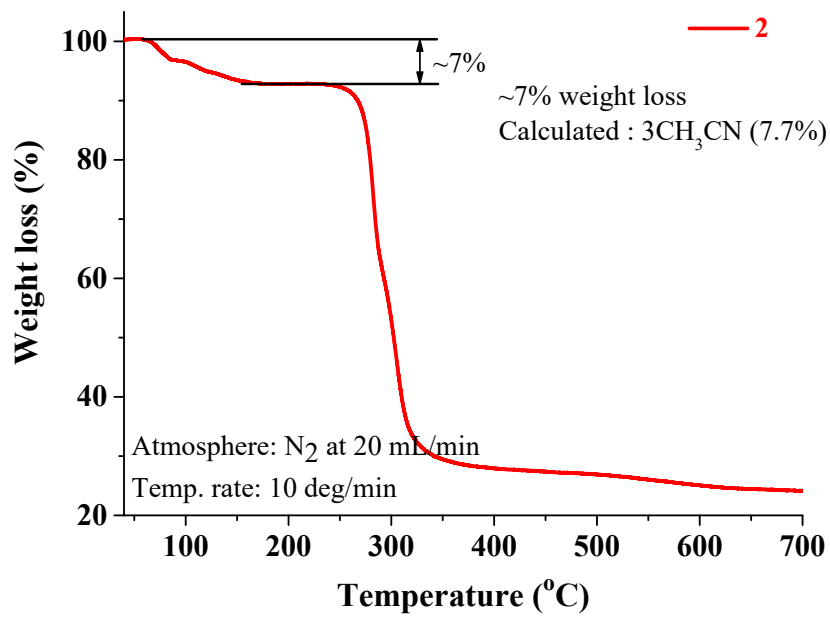


Figure S10. The TGA trace of complex 2.

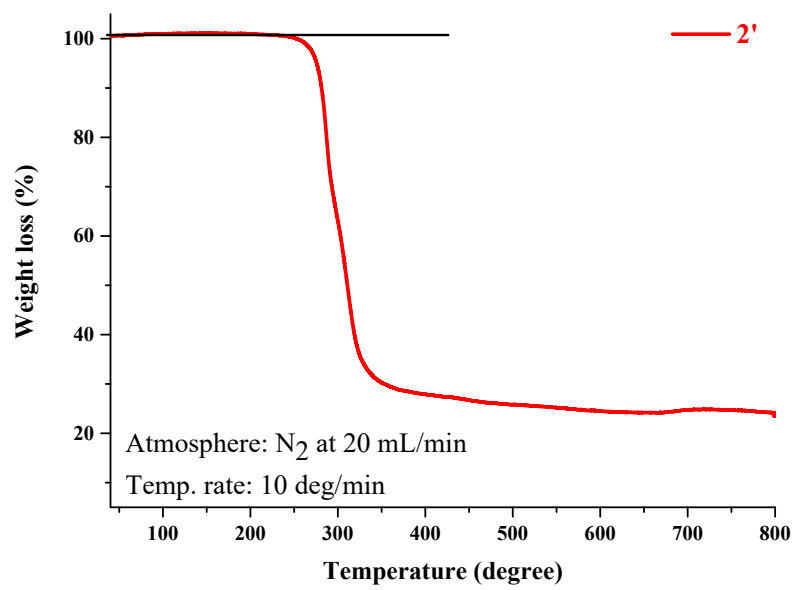


Figure S11. The TGA trace of complex 2'.

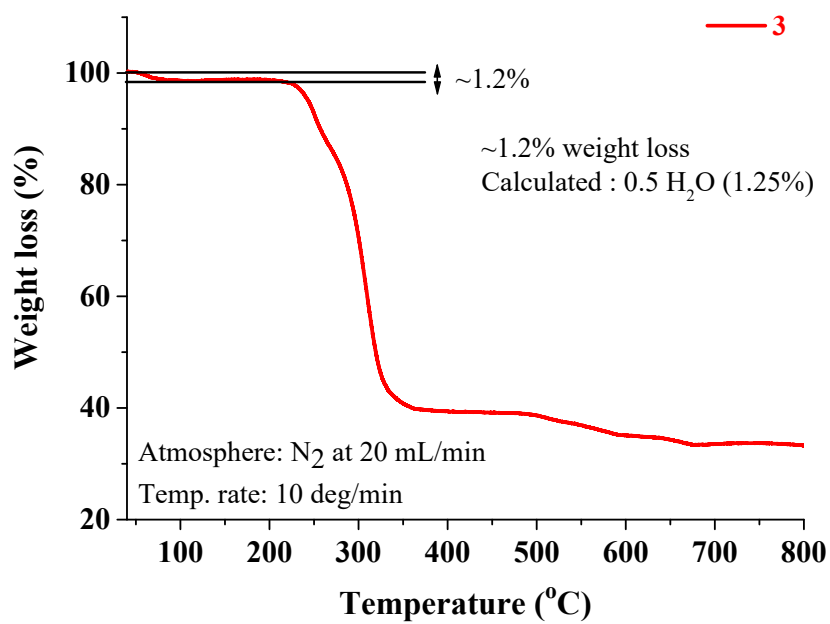


Figure S12. The TGA trace of complex 3.

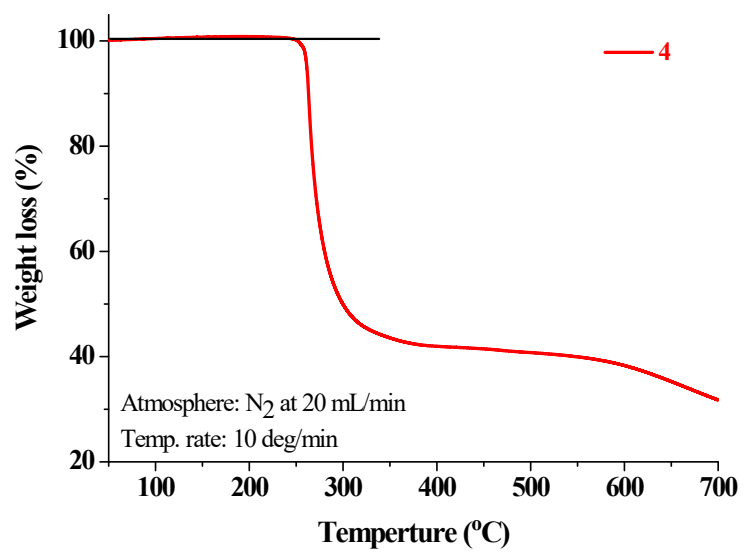


Figure S13. The TGA trace of complex 4.

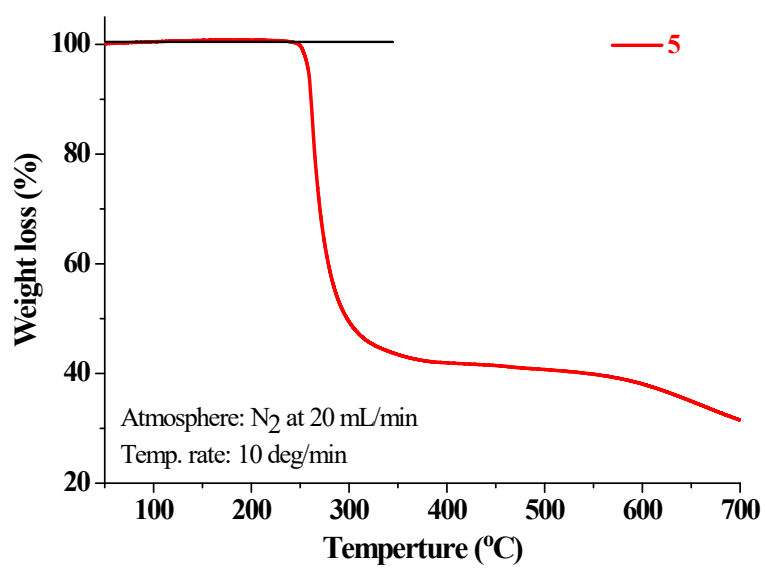


Figure S14. The TGA trace of complex 5.

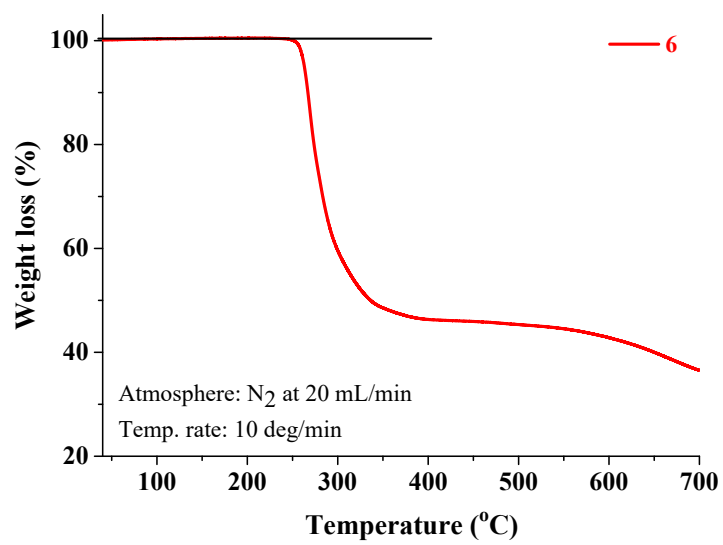


Figure S15. The TGA trace of complex **6**.

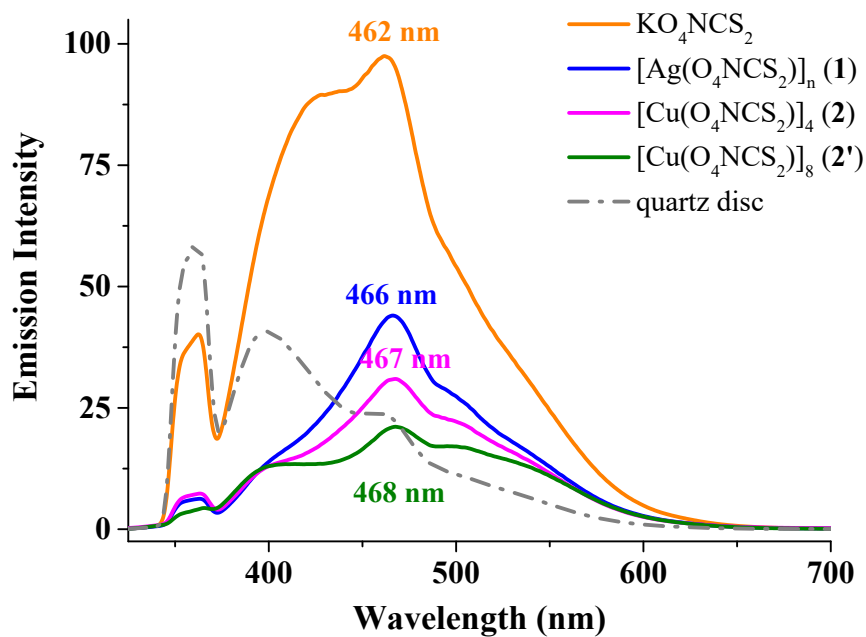


Figure S16. Luminescence spectra for solid samples of KO_4NCS_2 (orange line), complexes **1** (blue line), **2** (pink line), and **2'** (green line) and quartz disc (background : gray dash dotted line) at room temperature. The excitation wavelength is 350 nm.

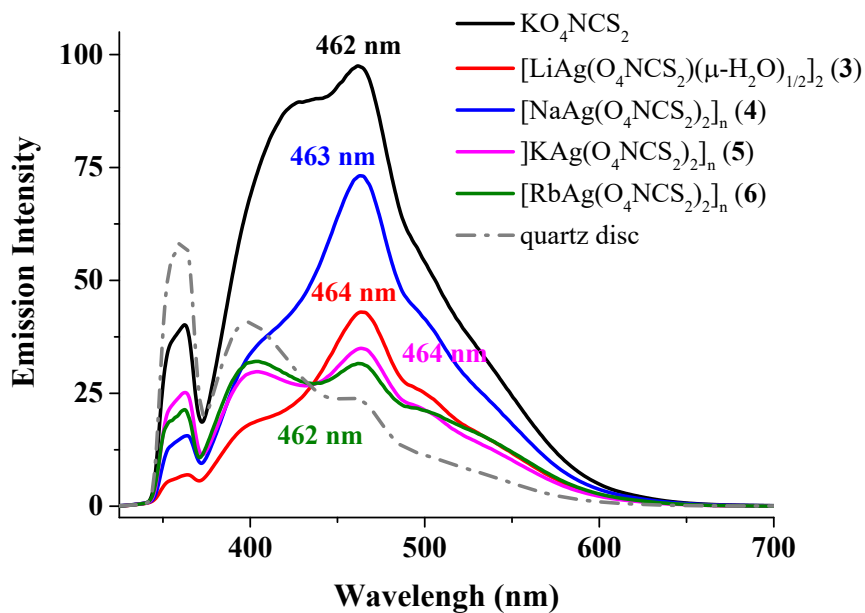


Figure S17. Luminescence spectra for solid samples of KO_4NCS_2 (purple line), complexes **3** (red line), **4** (blue line), **5** (pink line), and **6** (green line) and quartz disc (background : gray dash dotted line) at room temperature. The excitation wavelength is 350 nm.